

Chemical Reduction Behavior of Zirconia Doped to Nickel at Different Temperature in Carbon Monoxide Atmosphere

Norliza Dzakaria^{1,2,*}, Maratun Najihah Abu Tahari¹, Fairous Salleh¹, Alinda Samsuri³, Masitah Abdul Halim Azizi⁴, Tengku Shafazila Tengku Saharuddin⁵, Muhammad Rahimi Yusop¹, Wan Nor Roslam Wan Isahak⁴, Mohamed Wahab Mohamed Hisham¹, and Mohd Ambar Yarmo¹

¹Catalyst Research Group, School of Chemical Sciences and Food Technology, Faculty of Science and Technology, Universiti Kebangsaan Malaysia, 43600 UKM Bangi, Selangor Darul Ehsan, Malaysia

²School of Chemistry and Environment, Faculty of Applied Sciences, Universiti Teknologi MARA, Cawangan Negeri Sembilan, Kampus Kuala Pilah, Pekan Parit Tinggi, 72000 Kuala Pilah, Negeri Sembilan, Malaysia

³Department of Chemistry, Centre for Defence Foundation Studies, Universiti Pertahanan Nasional Malaysia, Kem Sungai Besi, 57000 Kuala Lumpur, Malaysia

⁴Department of Chemical and Process Engineering, Faculty of Engineering and Built Environment, Universiti Kebangsaan Malaysia, 43600 UKM Bangi, Selangor Darul Ehsan, Malaysia

⁵Faculty of Science and Technology, Universiti Sains Islam Malaysia, Bandar Baru Nilai, 71800, Nilai, Negeri Sembilan, Malaysia

* Corresponding author:

tel: +6019-7691734

email: norlizardzakaria75@gmail.com

Received: August 3, 2018

Accepted: December 11, 2018

DOI: 10.22146/ijc.40891

Abstract: The reduction behavior of nickel oxide (NiO) and zirconia (Zr) doped NiO (Zr/NiO) was investigated using temperature programmed reduction (TPR) using carbon monoxide (CO) as a reductant and then characterized using X-ray diffraction (XRD), nitrogen absorption isotherm using BET technique and FESEM-EDX. The reduction characteristics of NiO to Ni were examined up to temperature 700 °C and continued with isothermal reduction by 40 vol. % CO in nitrogen. The studies show that the TPR profile of doped NiO slightly shifts to a higher temperature as compared to the undoped NiO which begins at 387 °C and maximum at 461 °C. The interaction between ZrO₂ with Ni leads to this slightly increase by 21 to 56 °C of the reduction temperature. Analysis using XRD confirmed, the increasing percentage of Zr from 5 to 15% speed up the reducibility of NiO to Ni at temperature 550 °C. At this temperature, undoped NiO and 5% Zr/NiO still show some crystallinity present of NiO, but 15% Zr/NiO shows no NiO in crystalline form. Based on the results of physical properties, the surface area for 5% Zr/NiO and 15% Zr/NiO was slightly increased from 6.6 to 16.7 m²/g compared to undoped NiO and for FESEM-EDX, the particles size also increased after doped with Zr on to NiO where 5% Zr/NiO particles were 110 ± 5 nm and 15% Zr/NiO 140 ± 2 nm. This confirmed that the addition of Zr to NiO has a remarkable chemical effect on complete reduction NiO to Ni at low reduction temperature (550 °C). This might be due to the formation of intermetallic between Zr/NiO which have new chemical and physical properties.

Keywords: nickel; carbon monoxide; zirconia; reduction; temperature programmed reduction

■ INTRODUCTION

Nickel oxide has been used as a well-established catalyst due to its surface oxidation properties [1]. It is known that catalysis is a surface effect in which the

catalyst needs to provide the highest possible active surface area [2]. The reduction of metallic oxides to metal has been extensively studied as it represents a class of heterogeneous reactions which are of considerable

technological and commercial important [3]. Reduction of nickel oxide by hydrogen was studied by several researchers [4-7]. On the other hand, the study in the reduction of nickel oxide using carbon monoxide is limited due to the high possibility of carbide forming that may cause the reaction to be disturbed or retarded. Doping methods have been extensively utilized to modify the electronic structures of nanoparticles to achieve new or improved catalytic, electro-optical, magnetic, chemical, and physical properties [8-9]. The reduction of undoped and doped NiO catalysts has been studied extensively and plays an important role in many catalytic reactions [10].

Moreover, the addition of Zr to NiO enhances the catalytic activity and stability of NiO by improving oxygen storage capacity, reducibility, and resistance to sintering effect. ZrO₂ is an attractive material for catalysis known for its unique reducing, oxidizing, acidic and basic properties [11]. The reducing properties of ZrO₂ play an important role in the support effects [12]. The purpose of the present work is to enhance the reduction behavior by studying the influence of different concentrations of zirconia doping agents and their reduction behavior at different temperatures.

■ EXPERIMENTAL SECTION

Materials

Nickel oxide (99%) was obtained from Acros Organics, zirconyl chloride octahydrate (98%), Cl₂OZr·8H₂O from Acros Organics and ethanol, C₂H₆O (99.5%) from System[®] are pure and used as supplied. Gas mixture CO/N₂ (40% CO) was obtained from MOX.

Instrumentation

Temperature programmed reduction (TPR) measurements were collected by using Micromeritics Autochem 2920 Chemisorption Analyzer fed with 40% CO in N₂ at the flow rate of 20 mL min⁻¹ (STP) as reducing gas. Fifty milligrams of sample was heated up to three different maximum temperature 350, 450, and 550 °C, at a rate of 10 °C/min. The carbon monoxide consumption was monitored using a thermal conductivity detector (TCD). Phase characterization was carried out by X-ray

diffraction (XRD) model Bruker AXS D8 Advance type with X-ray radiation source of Cu Kα (40 kV, 40 mA) to record the 2θ diffraction angle from 10–80° (λ = 0.154 nm) to observe the crystallinity lattice structures of the catalyst samples. In order to identify the crystalline phase composition, the diffraction patterns obtained were matched with standard diffraction (JCPDS) files. In addition, FESEM images were obtained with Zeiss Merlin operating at 20 kV for morphological investigation of the catalysts. A ZEISS MERLIN Compact microscope equipped with a field emission gun and EDX probe was employed. Physical surface analysis of nitrogen adsorption at 77 K (liquid nitrogen) was conducted using a Micromeritics ASAP 2020 instrument to obtain the isotherm of each sample. The Brunauer–Emmett–Teller (BET) formula to get surface area technique was used to calculate the surface area, pore volume, and pore size [14]. The calcined samples of undoped NiO, 5% Zr/NiO and 15% Zr/NiO amounting to 100–300 mg were degassed at 300 °C for 4 h prior to the BET surface area analyses.

Catalyst Preparation

Two different concentrations of Zr doped nickel oxide: 5 and 15% w/w were prepared through the impregnation method. The impregnation method was prepared by using zirconyl chloride octahydrate (Cl₂OZr·8H₂O) and nickel oxide (NiO) powder. The amount of zirconia added was 5 and 15 w/w % of total metal cations. The compounds were dissolved in water followed by adding ethanol at 40 °C with stirring for 4 h which produced a viscous mixture. The solution was evaporated to dry while stirring for 4 h. It was then dried at 120 °C overnight followed by calcination in the air at 400 °C for 4 h [13]. The NiO samples with Zr were denoted as 5% Zr/NiO and 15% Zr/NiO while sample without Zr was denoted as NiO.

■ RESULTS AND DISCUSSION

Thermochemistry

The reduction reaction of nickel oxide using carbon monoxide environment follows the chemical equation NiO(s) + CO(g) → Ni(s) + CO₂ (g) and the

reduction of zirconia oxide by carbon monoxide follows the chemical equation $\text{ZrO}_2(\text{s}) + 2\text{CO}(\text{g}) \rightarrow \text{Zr}(\text{s}) + 2\text{CO}_2(\text{g})$. The thermodynamic quantities for NiO and ZrO_2 reduction by carbon monoxide are shown in Table 1. The Gibbs free energy change (ΔG_r) showed that the reduction of NiO to Ni is favorable and it occurred spontaneously at $\Delta G_r = -48 \text{ kJ}\cdot\text{mol}^{-1}$. The calculated ΔG_r became very negative from -48 to -50 $\text{kJ}\cdot\text{mol}^{-1}$ when the temperature increased from 350 to 550 °C. This showed that the reaction might occur more spontaneously at a higher temperature. Unlike the reduction of NiO to Ni, the reduction of ZrO_2 to Zr is not favorable which might due to the value of $\Delta G_r = +524 \text{ kJ}\cdot\text{mol}^{-1}$ which is positive. The calculated ΔG_r became less positive as the temperature increased, but it is still very positive to induce the reaction. The combination of NiO and ZrO_2 increased the reduction temperature due to the difficulty of zirconia oxide to reduce.

Adsorption Isotherm of N_2

The BET specific areas, average pore size and average pore volume of undoped ZrO_2 and NiO and doped NiO with 5 and 15 mol % Zr samples are summarized in Table 2. The isotherm of the samples is shown in Fig. 1. The catalysts showed type IV isotherm, which is typical for mesoporous materials (1.5–100 nm pore diameter) [14]. Table 2 shows that the BET surface area of NiO and ZrO_2 are 4.6 and 39.0 m^2/g , respectively, while BET surface area of doped NiO with 5 and 15% Zr

are 11.2 and 21.3 m^2/g , respectively. The catalysts have a low surface area due to high crystallinity. It was found that the surface area increased with increased loading of Zr to NiO which is in agreement with Salleh et al. [13] as ZrO_2 has higher BET surface areas than NiO. This suggested that there are more active sites that might be attributed to the higher temperature reduction of NiO after doping. Moreover, Wang et al. [15] suggested in their report that the specific surface area for metal oxide is one of the important factors in a chemical reaction. NiO surface coordination sites were exposed to the reduction gas when a specific surface area is higher. Thus, higher specific surface area provided the best result in reducibility of the nickel oxide. The addition

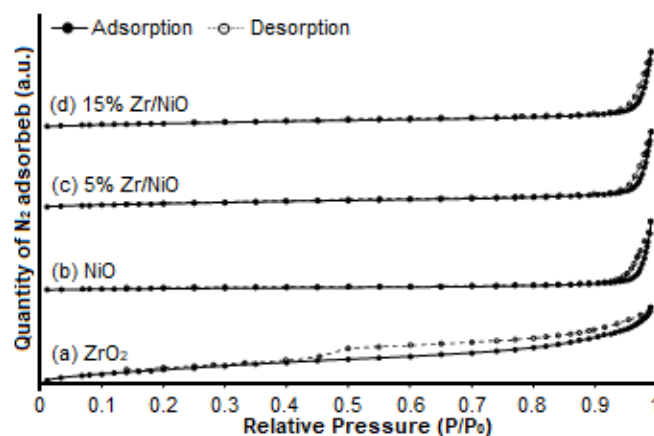


Fig 1. Nitrogen adsorption-desorption isotherms plot of undoped ZrO_2 and NiO and doped NiO with 5 and 15 mol % Zr catalyst

Table 1. Thermodynamic calculation for formation of nickel and zirconium

Reaction	Enthalpy, ΔH_r $\text{kJ}\cdot\text{mol}^{-1}$	Entropy, ΔS_r $\text{kJ}\cdot\text{mol}^{-1} \text{K}^{-1}$	ΔG_r 350 °C $\text{kJ}\cdot\text{mol}^{-1}$	ΔG_r 450 °C $\text{kJ}\cdot\text{mol}^{-1}$	ΔG_r 550 °C $\text{kJ}\cdot\text{mol}^{-1}$
Nickel oxide reduction	-43	+8	-48	-49	-50
Zirconia reduction	+535	+17	+524	+523	+521

Table 2. BET analysis of undoped ZrO_2 and NiO and doped NiO with 5 and 15 mol % Zr

Catalyst	BET surface area (m^2/g)	Average pore size (nm)	Average pore volume (cm^3/g)
ZrO_2	39.0	5.90	0.062
NiO	4.6	40.6	0.047
5% Zr/NiO	11.2	17.5	0.054
15% Zr/NiO	21.3	8.1	0.050

of Zr to NiO significantly increased the BET surface area of NiO due to the formation of new external pore on the NiO surface. In addition, the average pore size of undoped NiO was 40.6 nm, and the pore sizes of doped NiO with 5 and 15% Zr were decreased to 17.5 and 8.1 nm, respectively. The pore volume of undoped NiO was 0.047 cm³/g and decreased from 0.054 to 0.050 cm³/g when the concentration of Zr was increased from 5 to 15%. In this case, it is more likely that the Zr atoms had occupied the NiO mesopores which resulted in the average pore volume reduced when the concentration of Zr was increased.

Catalyst Characterization by TPR

The TPR patterns of non-isothermal 40% CO reductant for ZrO₂, NiO, 5% Zr/NiO and 15% Zr/NiO are shown in Fig. 2. The overall reactions involved a reaction between two different percentage of in mol of Zr/NiO, NiO, and ZrO₂ with carbon monoxide as reductant gas in a gas-solid reaction. The TPR profiles of ZrO₂ showed no peak. Meanwhile, NiO obviously showed one sharp peak that which indicates the reduction of ZrO₂ does not occur below 700 °C. The reduction process uses a one-step reduction profile, temperature region around 387 °C represents the reduction of NiO → Ni. Whereas, for 5% Zr/NiO, the reduction temperature shifted slightly to the right at around 406 °C. While 15% Zr/NiO, the reduction temperature shifted to a higher temperature at around

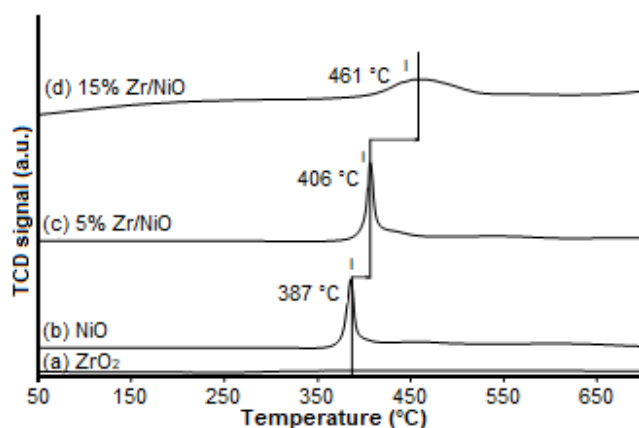


Fig 2. TPR profile of (a) undoped ZrO₂; (b) undoped NiO; (c) 5% Zr/NiO, and (d) 15% Zr/NiO samples (obtained after reduction at 400 °C for 4 h) under 40 vol.% CO at 40–700 °C

461 °C. There is a trace of NiO and Ni observed in the XRD analysis throughout the reduction process at the specified temperature; the peaks are attributed to state that the reduction process is incomplete. Furthermore, the addition of Zr element to NiO would delay the reduction process to a higher temperature and complete at above 550 °C.

Crystallinity Analysis using XRD

The XRD patterns of undoped ZrO₂ and NiO and doped NiO with 5 and 15 mol % Zr obtained after calcination at 400 °C for 4 h are shown in Fig. 3. The diffractogram of these samples was identical to the ZrO₂ phase (zirconia oxide, JCPDS 37-1484) and cubic NiO phase (nickel oxide, JCPDS 00-047-1049). The 2θ values revealed that the contribution of NiO main peaks was at 37.2, 43.4, 62.9, 75.5, and 79.5°. Furthermore, the diffractogram of 5 and 15% Zr/NiO showed no additional peak which suggested that the Zr particles loaded on the NiO are well dispersed. In addition, there is a reduction in the crystallinity of the prepared 5% Zr/NiO and 15% Zr/NiO when it is loaded with Zr, which is corresponded to the smaller NiO peaks intensity. This is due to the surface of NiO was covered or well dispersed by Zr atoms which are in amorphous form. No Zr peak was detected in the diffractogram due to Zr is in a highly amorphous form or well dispersed on the surface. Zr is in nanoparticles form that can be detected

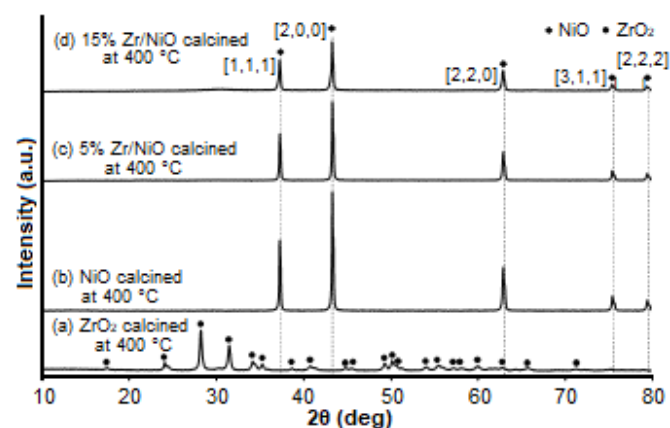


Fig 3. XRD patterns of (a) undoped ZrO₂; (b) undoped NiO; (c) 5% Zr/NiO and (d) 15% Zr/NiO samples obtained after calcination at 400 °C for 4 h

in the range of $0.1\text{--}1.0^\circ$ for wide scan in XRD analysis [16].

In order to investigate the role of Zr in the reduction process of NiO in CO atmospheres, all samples were collected at various reduction temperatures, i.e.: (i) 350, (ii) 450, and (iii) 550 °C for comparison purposes. The characterization using XRD as shown in Fig. 4 at different percent Zr element does give influence on the reduction of NiO in CO atmosphere. The reduction of undoped NiO and doped NiO with 5 and 15 mol % Zr were found to have different results. The diffractogram patterns for these samples at 350 °C showed strong peaks of crystallite cubic phase NiO [1,1,1], NiO [2,0,0], NiO [2,2,0], NiO [3,1,1] and NiO [2,2,2] (JCPDS 00-047-1049). All samples showed the formation of crystallite cubic phase NiO and Ni⁰ [1,1,1], Ni⁰ [2,0,0], Ni⁰ [2,2,0] (JCPDS 01-071-4654) as the temperature is approaching 450 °C. This suggested that the reduction process was initiated. However, as the temperature reached to 550 °C, 15% Zr/NiO sample showed only metallic Ni peaks which implied that the reduction process was completed. This result is contrary to the results of undoped NiO and 5% Zr/NiO samples in which these samples still consists of remaining crystalline phases of NiO. It suggested that there was a change in the properties of solid surface that particularly generates new active sites and promotes a strong modification to the behavior of the catalyst. In addition, the nature of the sample itself is also important, which in this case, the involvement of zirconia element in the structure of nickel oxide may contribute to the enhancement of reducibility process.

The additional Zr does give some advantages as illustrated in Fig. 5. From the illustration, the addition of 15% Zr to NiO completed the reduction of NiO → Ni at 550 °C but for undoped NiO, there was still a residue of NiO which was not reduced to Ni. In addition, based on the observations, we can anticipate that the catalyst has encountered some physical and chemical changes as shown in Fig. 6 with different temperatures for three samples producing different percentages of NiO reduction.

Surface Morphology by FESEM-EDX

Catalyst morphology was investigated by using

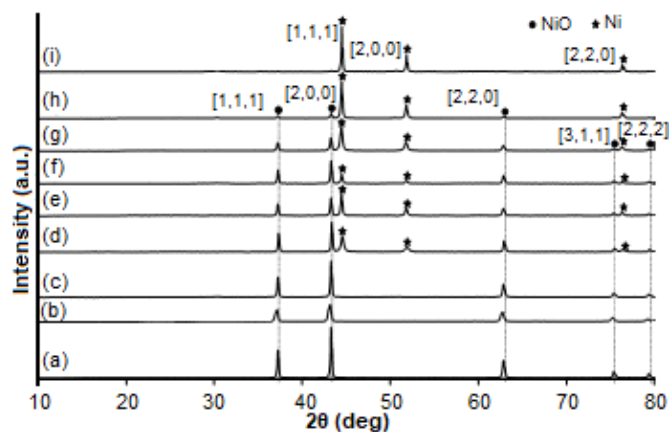


Fig 4. XRD patterns of non-isothermal reduction of undoped NiO and doped NiO with 5 and 15 mol % Zr catalyst using 40% CO in N₂. Note: (a) NiO after reduction 350 °C; (b) 5% Zr/NiO after reduction 350 °C; (c) 15% Zr/NiO after reduction 350 °C; (d) NiO after reduction 450 °C; (e) 5% Zr/NiO after reduction 450 °C; (f) 15% Zr/NiO after reduction 450 °C; (g) NiO after reduction 550 °C; (h) 5% Zr/NiO after reduction 550 °C; (i) 15% Zr/NiO after reduction 550 °C samples with 40 vol.% CO in nitrogen

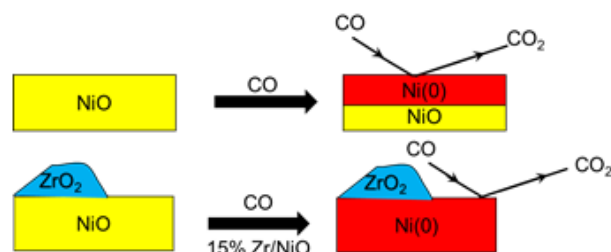


Fig 5. Proposed schematic sketch of CO interaction with undoped NiO and 15% Zr/NiO during reduction process in CO atmosphere

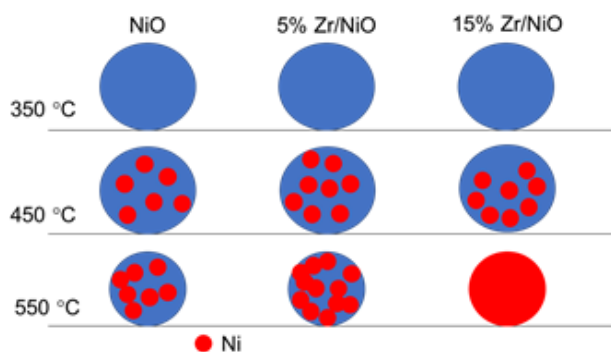


Fig 6. Graphical assumption of reduction for undoped NiO and doped NiO with 5 and 15 mol % Zr in CO atmosphere

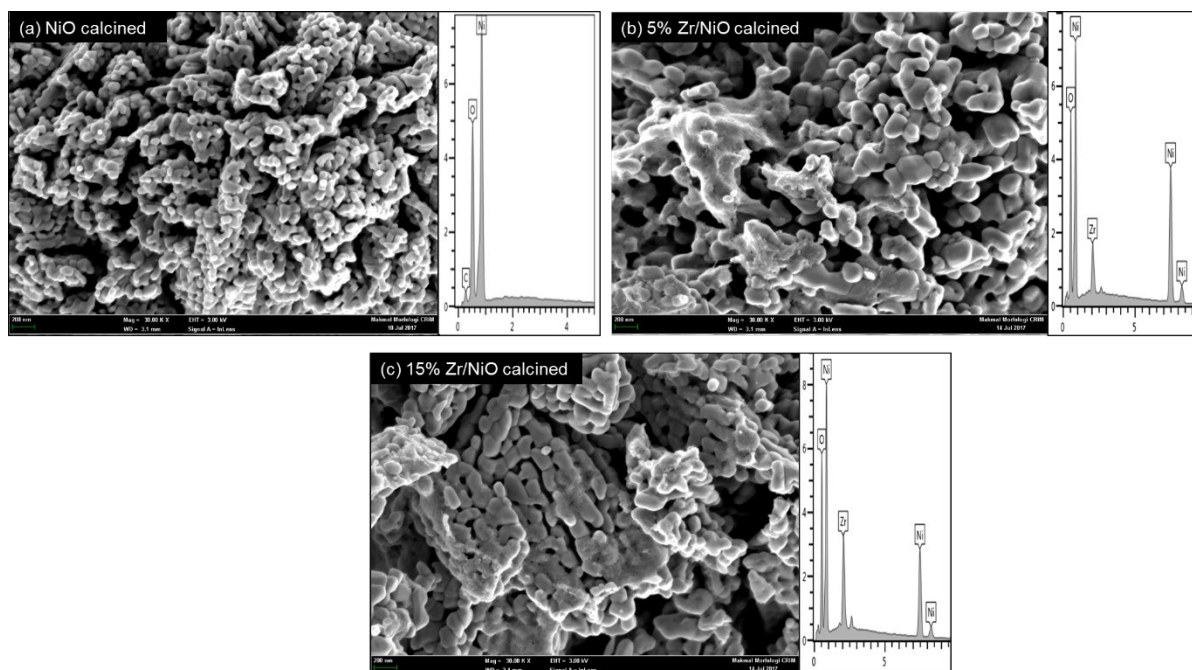


Fig 7. FESEM images of zirconia doped nickel oxide (a) Undoped NiO; (b) Doped NiO with 5 mol % Zr; (c) Doped NiO with 15% Zr (Magnification: 30K x) after calcined at 400 °C for 4 h

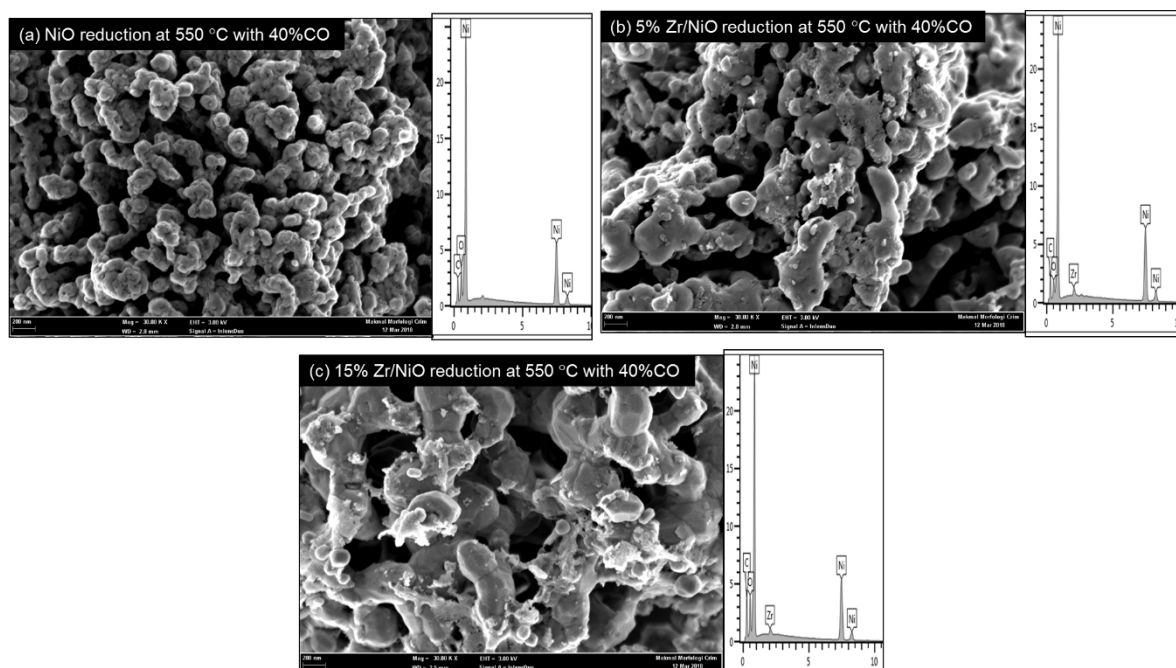


Fig 8. FESEM images of zirconia doped nickel oxide (a) Undoped NiO; (b) Doped NiO with 5 mol % Zr; (c) Doped NiO with 15 mol % Zr (Magnification: 30K x) after reduction with 40% CO in nitrogen

FESEM and the results are shown in Fig. 7. The NiO catalyst was observed as a rod structure. The addition of Zr to NiO altered the morphology significantly. The morphology of NiO catalysts was influenced by the Zr.

Doped NiO with 5 and 15 mol % Zr catalysts exhibited irregular shape and non-uniform particle size distribution. The structure and morphology of the catalyst were influenced by doped metal oxide [17].

Compare to undoped NiO, the particle size is smaller than doped NiO with 5 and 15 mol % Zr. The average sizes of the undoped NiO and doped NiO with 5 and 15 mol % Zr were measured by using the Scion image program averaged over 100 particles. The average sizes of the undoped NiO were found to be 45 ± 5 nm, while doped NiO with 5 mol % Zr particles 110 ± 5 nm and doped NiO with 15 mol % Zr/NiO 140 ± 2 nm. These numbers showed that there is a change in the particle size due to the loading of big particles such as Zr. As an exhibit in Fig. 8, it is observed that at reduction temperature of 550 °C, the particle size of undoped NiO and doped NiO with 5 mol % Zr remain the same. Meanwhile, the doped NiO with 15 mol % Zr particle size was increased due to the formation of Ni metal. This result showed the formation of metallic Ni after reduction of doped NiO with 15 mol % Zr with CO contributed in the formation of agglomeration of particle surfaces which is in agreement with Zielinska et al. [18] report. Furthermore, the agglomeration will increase the availability of the surface area and thus influences the rate of the reduction process.

■ CONCLUSION

Analysis by TPR showed the addition of Zr has a remarkable influence on the reduction process where the peak is shifted to the right from lower to higher temperature (387 to 461 °C). Zr dopant enhances the reduction process with the reduction completed at temperature 550 °C with only metallic phase detected by XRD compared to undoped NiO and doped NiO with 5 mol % Zr which has residue NiO detected. This is due to the catalytic effect of doped NiO with 15 mol % Zr. Therefore, Zr species played an important role in enhancing the reduction of NiO by completing the reduction at temperature 550 °C, due to Zr particles were fully dispersed on the NiO surface. Moreover, the addition of Zr to NiO provides higher surface area, and for FESEM the particles size become larger as with the increase of Zr concentration.

■ ACKNOWLEDGMENTS

The author wishes to thank the Ministry of Higher Education (MOHE), research grants ST-2018-005

(MTJA) and Centre of Research and Innovation Management CRIM-UKM for instrumentation facilities.

■ REFERENCES

- [1] Rahim, M.A.A., Hameed, R.M.A., and Khalil, M.W., 2004, Nickel as a catalyst for the electro-oxidation of methanol in alkaline medium, *J. Power Sources*, 134 (2), 160–169.
- [2] Antolini, E., 2003, Formation of carbon-supported PtM alloys for low temperature fuel cells: A review, *Mater. Chem. Phys.*, 78 (3), 563–573.
- [3] Ostyn, K.M., and Carter, C.B., 1982, On the reduction of nickel oxide, *Surf. Sci.*, 121 (3), 360–374.
- [4] Syed-Hassan, S.S.A., and Li, C.Z., 2011, NiO reduction with hydrogen and light hydrocarbons: Contrast between SiO₂-supported and unsupported NiO nanoparticles, *Appl. Catal., A*, 398 (1-2), 187–194.
- [5] Chatterjee, R., Banerjee, S., Banerjee, S., and Ghosh, D., 2012, Reduction of nickel oxide powder and pellet by hydrogen, *Trans. Indian Inst. Met.*, 65 (3), 265–273.
- [6] Jeangros, Q., Hansen, T.W., Wagner, J.B., Damsgaard, C.D., Dunin-Borkowski, R.E., Hébert, C., Van Herle, J., and Hessler-Wyser, A., 2013, Reduction of nickel oxide particles by hydrogen studied in an environmental TEM, *J. Mater. Sci.*, 48 (7), 2893–2907.
- [7] Manukyan, K.V., Avetisyan, A.G., Shuck, C.E., Chatilyan, H.A., Rouvimov, S., Kharatyan, S.L., and Mukasyan, A.S., 2015, Nickel oxide reduction by hydrogen: Kinetics and structural transformations, *J. Phys. Chem. C*, 119 (28), 16131–16138.
- [8] Liao, L., Mai, H.X., Yuan, Q., Lu, H.B., Li, J.C., Liu, C., Yan, C.H., Shen, Z.X., and Yu, T., 2008, Single CeO₂ nanowire gas sensor supported with Pt nanocrystals: Gas sensitivity, surface bond states, and chemical mechanism, *J. Phys. Chem. C*, 112 (24), 9061–9065.
- [9] Koao, L.F., Swart, H.C., and Dejene, F.B., 2010, Effects of aluminum co-doping on

- photoluminescence properties of Ce³⁺-doped SiO₂ glasses, *J. Rare Earths*, 28 (Suppl. 1), 206–210.
- [10] Laosiripojana, N., Sutthisripok, W., and Assabumrungrat, S., 2005, Synthesis gas production from dry reforming of methane over CeO₂ doped Ni/Al₂O₃: Influence of the doping ceria on the resistance toward carbon formation, *Chem. Eng. J.*, 112 (1-3), 13–22.
- [11] Mekhemer, G.A.H., 1998, Characterization of phosphated zirconia by XRD, Raman and IR spectroscopy, *Colloids Surf., A*, 141 (2), 227–235.
- [12] Tanabe, K., 1985, Surface and catalytic properties of ZrO₂, *Mater. Chem. Phys.*, 13 (3), 347–364.
- [13] Salleh, F., Saharuddin, T.S.T., Samsuri, A., Othaman, R., and Yarmo, M.A., 2015, Effect of zirconia and nickel doping on the reduction behavior of tungsten oxide in carbon monoxide atmosphere, *Int. J. Chem. Eng. Appl.*, 6 (6), 389–394.
- [14] Brunauer, S., Emmett, P.H., and Teller, E., 1938, Adsorption of gases in multimolecular layers, *J. Am. Chem. Soc.*, 60 (2), 309–319.
- [15] Wang, C., Yin, L., Zhang, L., Xiang, D., and Gao, R., 2010, Metal oxide gas sensors: sensitivity and influencing factors, *Sensors*, 10, 2088–2106.
- [16] Pradhan, D., 2009, Unusual Phase Transformation Behavior of Amorphous Zirconia, *Thesis*, Department of Ceramic Engineering, National Institute of Technology Rourkela, India.
- [17] Namratha, K., and Byrappa, K., 2012, Novel solution routes of synthesis of metal oxide and hybrid metal oxide nanocrystals, *Prog. Cryst. Growth Charact. Mater.*, 58 (1), 14–42.
- [18] Zielińska, K., Stankiewicz, A., and Szczygieł, I., 2012, Electroless deposition of Ni-P-nano-ZrO₂ composite coatings in the presence of various types of surfactants, *J. Colloid Interface Sci.*, 377 (1), 362–367.